MIB1 Upregulates IQGAP1 and Promotes Pancreatic Cancer Progression by inducing ST7 Degradation

Tao Liu
Wuhan Union Hospital
Bin Zhang
Wuhan Union Hospital
xin jin (jinxinunion@hust.edu.cn)
Wuhan Union Hospital https://orcid.org/0000-0001-6461-6005
Xiang Cheng
Wuhan Union Hospital

Research

Keywords: MIB1, ST7, IQGAP1, pancreatic cancer

Posted Date: September 23rd, 2020

DOI: https://doi.org/10.21203/rs.3.rs-76668/v1

Abstract

Background

Pancreatic cancer is a highly heterogeneous and has a poor prognosis. Elucidating the molecular mechanisms underlying pancreatic cancer progression is essential for improving patient survival. Although the E3 ubiquitin ligase mind bomb 1 (MIB1) is involved in cancer cell proliferation and is often overexpressed in pancreatic cancer, the role of MIB1 in pancreatic cancer progression remains unclear.

Methods

The relationship of MIB1 with the clinicopathological features of pancreatic tumors was bioinformatically investigated in different datasets. The protein levels of MIB1 and ST7 were assessed by Western blotting and immunohistochemistry. The role of MIB1 and ST7 in pancreatic cancer growth was assessed by MTS assays, colony formation assays, and experiments in mouse xenograft models. The interaction between MIB1 and ST7 was investigated by co-immunoprecipitation. The relationship between MIB1, ST7, and IQGAP1 levels was explored by Western blotting and quantitative real-time PCR.

Results

MIB1 expression was elevated in pancreatic cancer tissues, and its expression levels were associated with unfavorable prognosis. MIB1 overexpression enhanced pancreatic cancer proliferation and invasion *in vitro* and *in vivo*. We identified ST7 as a novel MIB1 target for proteasomal degradation. Further, we found that ST7 suppressed tumor growth by downregulating IQGAP1 in pancreatic cancer cells.

Conclusions

These data suggest that MIB1 promotes pancreatic cancer progression by inducing ST7 degradation. ST7 suppresses tumor growth by downregulating IQGAP1 in pancreatic cancer cells. Therefore, the MIB1/ST7/IQGAP1 axis is essential for pancreatic cancer progression, and MIB1 inhibition may improve the survival of pancreatic cancer patients.

Background

Pancreatic cancer is a highly heterogeneous malignancy characterized by rapid growth, early metastasis, resistance to chemotherapy, and high mortality rate [1]. Genetic heterogeneity within tumors strongly affects numerous oncogenic signaling pathways, driving cancer evolution and resistance to treatment [2]. Mutations in *KRAS*, *TP53*, *CDKN2A*, and *SMAD4*, among other genes, have been linked to pancreatic cancer progression [3]. Despite recent progress in cancer therapeutics, the prognosis of pancreatic cancer patients remains extremely poor [4]. Therefore, elucidating the role of gene mutations and number alterations in pancreatic cancer pathogenesis is critical for improving the survival of pancreatic cancer patients.

Mind bomb 1 (MIB1) is an E3 ubiquitin ligase involved in various cellular processes [5]. The N-terminal of MIB1 contains 2 substrate recognition domains, whereas the C-terminal of MIB1 mediates the degradation of substrates containing multiple RING domains [5]. MIB1 has been shown to ubiquitinate Delta proteins, which are Notch ligands [5]. In addition to regulating Notch signaling, MIB1 ubiquitinates other critical signaling components, such as degrading PLK4 to regulate centriole biogenesis [6]. Although MIB1 overexpression has been reported in pancreatic cancer [7], the role of MIB1 in pancreatic cancer progression remains unclear.

KRAS mutations are found in 90% of pancreatic cancer patients [4]. Aberrant activation of the MAPK signaling pathway is a key driver of pancreatic cancer cell proliferation and metastasis [8]. IQGAP1 has been identified as a scaffold protein regulating numerous MAPK cascades [9]. We have recently shown that FBP1 binds the WW domain of IQGAP1, inhibiting ERK phosphorylation in pancreatic cancer cells [10]. Nevertheless, the mechanisms regulating IQGAP in pancreatic cancer are understudied. Herein, we show that ST7 is a bona fide substrate of MIB1. MIB1 promotes ST7 degradation via the ubiquitin-proteasome system. We also report that in pancreatic cancer, ST7 suppresses MIB1 expression. Finally, we show that the MIB1/ST7 axis modulates the expression of IQGAP1 in pancreatic cancer. The results presented herein suggest that MIB1 is a promising candidate target for pancreatic cancer therapy.

Materials And Methods

Cell lines, cell culture, and transfection

All pancreatic cancer cell lines (HPDE6-C7, PANC-1, BxPC-3，AsPC-1, SW1990, MIA PaCa-2) were purchased from the Chinese Academy of Science Cell Bank, as previously reported [11]. All cell lines were cultured in Dulbecco's modified Eagle's medium (Invitrogen, USA) containing 10% fetal bovine serum (FBS; HyClone, USA); cells were maintained in a 5% CO_2 and 37ºC incubator. Transfections were performed using Lipofectamine 2000 (Thermo Fisher Scientific). The lentivirus-based control and gene-specific shRNAs (shMIB1#1, shMIB1#2, shST7#1, shST7#2, Sigma-Aldrich) were employed to produce different lentiviral particles in 293T cells. Twenty-four hours after transfection, the cell culture medium was replaced with fresh Dulbecco's modified Eagle's medium (supplemented with 10% FBS and 1 mM sodium pyruvate). Subsequently, the cell culture medium containing the viral particles was collected after 48 hours and used to transduce pancreatic cancer cells after the addition of 12 μg/mL polybrene. Puromycin selection (10 μg/mL; 24 hours) was performed to eliminate non-infected cells. The sequences of the shRNAs used are provided in Supplementary Table S1.

Plasmids and reagents

Flag-MIB1，MIB1 N-terminal and MIB1 C-terminal plasmids was cloned into the CMV-MCS-3xFlag-SV40-neomycin vector by GENECHEM (Shanghai, China). KOD-Plus-Mutagenesis Kit (Cat #SMK-101B,

TOYOBO) was used to generate the Flag-MIB1ΔRING mutant. The following antibodies were used in this study: MIB1 (4400, Cell Signaling Technology; 1:1000 dilution), GAPDH (ab8245, Abcam; 1:5000 dilution), ST7 (ab122459, Abcam; 1:200 dilution), and IQGAP1 (20648, Cell Signaling Technology; 1:2000 dilution). The proteasome inhibitor MG-132 (Cat. No. S2619) was purchased from Selleckchem.

Co-immunoprecipitation and Western blot analysis

Ethical approval for the use of human tissues (12 pairs of matched pancreatic cancer and adjacent non-cancerous tissues) was obtained by the local ethics committee (Tongji Medical College, China), and written informed consent was obtained from all patients before surgery. For co-immunoprecipitation, cells were harvested and incubated in 1mL of RIPA buffer for 20 min on ice. Cell lysates were centrifuged at 12000 rpm for 15 min at 4ºC. The supernatant was collected and incubated with Pierce Protein G Agarose (Thermo Fisher Scientific, USA) and primary antibody or IgG in the cold room overnight. The beads were washed 5 times with RIPA buffer, resuspended with sample loading buffer, and heated at 100ºC for 5 min. The supernatant was used for Western blotting. Pancreatic cancer whole-cell lysates were obtained in RIPA buffer, freshly supplemented with 1 mM phenylmethanesulfonyl fluoride (PMSF). Protein concentration was determined by the BCA method. Equal amounts of protein were separated by SDS-PAGE and transferred onto PVDF membranes. Subsequently, membranes were incubated with primary antibodies for at least 8 hours at 4ºC. Next, membranes were probed with the appropriate secondary antibody for 1 hour at room temperature. Signals were detected using the Chemiluminescent Western Blot Detection Kit (cat. no. 32209, Thermo Fisher Scientific, USA).

Quantitative real-time PCR (qRT-PCR)

Total RNA from pancreatic cancer cells was extracted using TRIzol (Thermo Fisher Scientific, USA). Reverse transcription was conducted to generate cDNA (PrimeScript™ RT reagent Kit) reported previously [12]. qRT-PCR analysis was carried out using TB Green™ Fast qPCR Mix. Relative mRNA levels of target genes were calculated using the $2^{-\Delta\Delta Cq}$ method after normalization to *GAPDH* mRNA levels. The sequences of the forward and reverse primers for *MIB1, ST7, IQGAP1,* and *GAPDH* are provided in Supplementary Table S2.

In vitro cell growth assay

Pancreatic cancer cells (1×10^4) were seeded in 96-well plates, and MTS reagent was added according to the manufacturer's protocol (cat. no. ab197010, Abcam). Absorbance at 490 nm was measured to evaluate *in vitro* cell growth. For colony formation assay the cells were seeded into 6-well plates (500 cells/well) and incubated in prescribed medium with 10% FBS at 37°C. After cultured for 14 days, the cells were fixed in methanol for 30 min and stained with 1% Crystal Violet Staining Solution for 30 mins and then washed with PBS 3 times. Finally, the number of colonies was calculated.

In vitro invasion assay

The in vitro cell invasion assay was applied by using a Bio-Coat Matrigel invasion chamber (BD Biosciences) according to the protocol of the manufacturer. Cells were cultured in the insert for 24 h. Cells were fixed in methanol for 15 min and then stained with 1 mg/ml crystal violet for 20 min. At least three fields for each group of invaded cells were counted.

In vivo tumor growth assay

All animal procedures were approved by the Ethics Committee of Tongji Medical College, Huazhong University of Science and Technology. BALB/c-nude mice (4-5 weeks old, 18-20 g) were purchased from Vitalriver (Beijing, China). BxPC-3 cells were infected with the indicated lentiviral particles. After puromycin selection for 48 hours, cells (1×10^7 per mouse) were subcutaneously injected into the back of mice. The length and width of xenografts were measured using a Vernier caliper, and tumor volumes were calculated using the formula $(L \times W^2)/2$. After mice were euthanized, tumors were excised and weighted.

Tissue microarray and immunohistochemistry (IHC)

Tissue microarray (cat. no. XT14-029, Outdo Biobank, Shanghai, China) and IHC were performed to assess the levels of MIB1 in pancreatic ductal adenocarcinoma (PDAC), as well as the relationship between MIB1 and ST7. For IHC, the following antibodies were used: MIB1 (4400, Cell Signaling Technology; 1:400 dilution) and ST7 (ab122459, Abcam; 1:200 dilution). The IHC score was calculated based on the staining intensity and the proportion of positive tumor cells. The staining intensity was graded according to the following criteria: 1 = weak staining at 100x magnification and limited or no staining at 40x magnification; 2 = moderate staining at 40x magnification; 3 = strong staining at 40x magnification. Two experienced and blinded to the study pathologists independently scored the immunostaining intensity and determined the proportion of positive tumor cells.

Correlation analysis using GEPIA

Gene Expression Profiling Interactive Analysis (GEPIA, http://gepia.cancerpku.cn/index.html) online tool was used to analyze RNA sequencing data from The Cancer Genome Atlas (TCGA) and the Genotype-Tissue Expression (GTEx) databases. GEPIA performs survival analyses based on gene expression levels and uses a log-rank test for hypothesis evaluation. GEPIA also performs a pairwise gene correlation analysis for any given sets of TCGA and GTEx expression data using Pearson correlation statistics.

Statistical analysis

All data are presented as the means ± standard deviation (SD). Statistical significance was determined by one-way or two-way ANOVA using GraphPad Prism 5 software. *P*-values <0.05 were considered statistically significant.

Results

MIB1 overexpression is associated with poor prognosis in pancreatic cancer

To assess the relationship between MIB1 expression and clinicopathological characteristics in pancreatic cancer, we analyzed *MIB1* mRNA levels in the TCGA database and found that *MIB1* was upregulated in 16% of pancreatic cancers (Figure 1A). Consistently, we found that the mRNA levels of MIB1 were significantly higher in pancreatic cancer tissues (n = 179) than normal pancreatic tissue (n = 171) (Figure 1B). We also investigated the protein levels of MIB1 in pancreatic cancer specimens using tissue microarrays (n = 25 normal pancreatic tissues, n = 35 PDAC) and IHC. MIB1 protein levels were significantly higher in pancreatic cancer tissues than in normal pancreas ($P < 0.001$; Figure 1C, 1D). Western blot analysis of specimens from our hospital [11] confirmed the higher MIB1 protein levels in pancreatic cancer (n = 12) than in adjacent normal pancreatic tissues (n = 12) (Figure 1E, 1F). Moreover, we MIB1 expression levels were higher in pancreatic cancer cell lines than in non-malignant pancreatic ductal epithelial cells (HDPE6-C7; Figure 1G, 1H). These results strongly suggest that MIB1 is upregulated in pancreatic cancer. Importantly, high MIB1 expression levels in pancreatic cancer patients were associated with shorter overall survival by using The Human Protein atlas (Figure 1I), suggesting that aberrant MIB1 expression may represent a poor prognosis biomarker in pancreatic cancer.

MIB1 promotes pancreatic cancer cell growth and invasion

Next, we assessed the role of MIB1 in pancreatic cancer cell growth. To this end, we silenced MIB1 expression in BxPC-3 and SW1990 cells using 2 different shRNAs (Figure 2A, 2B), followed by MTS assay and colony formation analysis. MIB1 silencing significantly inhibited cancer cell proliferation (Figure 2C, 2D). Additionally, transwell assays revealed that MIB1 knockdown markedly impaired the invasion ability of cancer cells (Figure 2E, 2F). To determine the effects of MIB1 knockdown on pancreatic cell growth *in vivo*, we subcutaneously injected BxPC-3 cells (expressing shControl or shMIB1#1) in nude mice and assessed tumor growth. We found that MIB1 knockdown profoundly reduced tumor growth (Figure 2G-2I). Conversely, ectopic overexpression of MIB1 (Figure 2J, 2K) enhanced pancreatic cancer cell proliferation and invasion, both in BxPC-3 and SW1990 cells (Figure 2L, 2M). These findings indicate that MIB1 plays a critical role in pancreatic cancer progression.

MIB1 interacts with ST7 in pancreatic cancer cells

To explore the mechanisms underlying the pro-tumorigenic effects of MIB1 in pancreatic cancer, we performed immunoprecipitation and mass spectrometry to identify binding partners of MIB1 (Figure 3A, 3B, and Supplementary Table 1). Since MIB1 is an E3 ligase, we hypothesized that it promotes cancer development and progression by targeting tumor suppressor proteins for degradation. ST7 is known to suppress the growth of multiple solid tumor types, including prostate [13], gastric [14], and colorectal cancer [15]. In this study, we found that ST7 was one of the potential binding partners of MIB1 (Figure 3C). Co-immunoprecipitation results confirmed the interaction between MIB1 and ST7 in BxPC-3 and Sw1990 cells (Figure 3D, 3E). To identify the region of MIB1 responsible for its interaction with ST7, we constructed MIB1 N-terminal (amino acids 1-429) and MIB1 C-terminal (amino acids 430-1006) plasmids (Figure 3F). We found that the N-terminal domain of MIB1 was responsible for MIB1-ST7 interaction (Figure 3G).

ST7 is a bona fide substrate of MIB1 in pancreatic cancer

Given that MIB1 is an E3 ligase, we assessed whether MIB1 targets ST7 for degradation. We found that MIB1 knockdown increased the protein but not the mRNA level of ST7 in BxPC-3, SW1990, and AsPC-1 cells (Figure 4A, 4B). Conversely, MIB1 overexpression decreased ST7 protein levels in pancreatic cancer cell lines, although ST7 mRNA levels remained unchanged (Figure 4C, 4D). Interestingly, proteasome inhibition with MG132 in BxPC-3 cells abrogated the ability of MIB1 overexpression to decrease ST7 levels (Figure 4E). Since the RING domain is essential for the E3 ligase activity of MIB1, we constructed a MIB1-ΔRING mutant, which lacked the RING domain. Although the expression of wild-type MIB1 decreased ST7 levels in BxPC-3 cells, expression of the MIB1-ΔRING mutant failed to do so (Figure 4F). We also found that MIB1 repression prolonged the half-life of ST7 protein (Figure 4G) and reduced the polyubiquitination levels of ST7 in BxPC-3 cells (Figure 4I). Conversely, the protein half-life of ST7 in MIB1 overexpressing cells was shorter than that in the control group (Figure 4H). Furthermore, overexpression of wild-type MIB1 increased the polyubiquitination levels of ST7, although expression of the MIB1ΔRING mutant did not alter the levels of ST7 polyubiquitination in BxPC-3 cells. We also examined the protein levels of ST7 and MIB1 in a pancreatic cancer tissue microarray (n = 35 samples). We found a negative correlation between MIB1 and ST7 protein levels in pancreatic cancer tissues (Pearson correlation r = -0.3535, P = 0.0372; Figure 4K.). Together, these data indicate that MIB1 promotes ST7 polyubiquitination and proteasomal degradation in pancreatic cancer.

ST7 plays a key role in MIB1-induced pancreatic cancer cell growth

Although ST7 has been reported to have tumor suppressor functions in multiple cancer types, its role in pancreatic cancer remains unknown. MTS and colony formation assays revealed that ST7 silencing by 2 different siRNAs (Figure 5A, 5B) markedly increased cell growth, both in BxPC-3 and SW1990 cells (Figure 5C, 5D). Similarly, ST7 knockdown enhanced pancreatic cancer cell invasion *in vitro* (Figure 5E). These

findings suggest that ST7 acts as a tumor suppressor in pancreatic cancer. To assess the relevance of ST7 in the tumor-promoting effects of MIB1 in pancreatic cancer, we used BxPC-3 cells expressing shControl, shMIB1, shST7, and shMIB1/shST7 (Figure 5F, 5G). ST7 silencing increased tumor growth, and MIB1 silencing alone inhibited the proliferation of BxPC-3 cells (Figure 5H-5K). Notably, combined silencing of ST7 and MIB1 diminished the anti-proliferative effects of MIB1 downregulation *in vitro* and *in vivo* (Figure 5H-5K). These results suggest that MIB1 promotes pancreatic cancer progression by targeting ST7 for degradation.

The MIB1/ST7/IQGAP1 signaling axis promotes pancreatic cancer proliferation

To get further insight into the anti-tumor effects of ST7 in pancreatic cancer, we performed RNA-seq analysis in BxPC-3 cells with or without ST7 silencing (Figure 6A and 6B). KEGG pathway enrichment analysis of the differentially expressed genes demonstrated that ST7 knockdown upregulated numerous genes involved in the actin cytoskeleton pathway (Figure 6C). Importantly, ST7 silencing significantly upregulated IQGAP1, which has been shown to promote pancreatic cancer proliferation [10]. We conducted Western blotting and qRT-PCR analysis and confirmed that ST7 knockdown increased the protein and mRNA levels of IQGAP1, respectively; this finding was consistent in BxPC-3 and SW1990 cells (Figure 6D, 6E). Additionally, IQGAP1 silencing alone suppressed cell growth in BxPC-3 and SW1990 cells (Figure 6F). The ability of ST7 silencing to increase pancreatic cancer cell growth was attenuated by the combined silencing of IQGAP1 and ST7 (Figure 6F). These results suggest an essential role for IQGAP1 in the anti-tumor effects of ST7 in pancreatic cancer.

Next, we silenced ST7, IQGAP1, and ST7/IQGAP1 expression in BxPC-3 cells. MIB1 knockdown decreased IQGAP1 expression levels; however, double knockdown of MIB1 and ST7 abolished the ability of MIB1 to regulate IQGAP1 expression (Figure 6G, 6H). MIB1 overexpression upregulated IQGAP1 in BxPC-3 cells, both at the protein and mRNA levels (Figure 6I, 6J). Consistently, ST7 knockdown abrogated the MIB1-mediated IQGAP1 upregulation (Figure 6I and 6J). Together, these data suggest that MIB1 targets ST7 for degradation, thereby increasing IQGAP1 expression levels and promoting pancreatic cancer progression (Figure 6K).

Discussion

ST7 mutations have been reported in breast, colon, esophagus, and gastric cancers [14, 16, 17]. Additionally, ST7 overexpression has been shown to suppress the *in vivo* tumorigenicity PC-3 prostate cancer cells [16], suggesting that ST7 has tumor suppressor functions [18]. However, the precise mechanisms underlying the anti-tumor effects of ST7 are poorly understood. Previously studies have shown that ST7 suppressed tumor growth by modulating the expression of genes involved in cellular structure and architecture [18]. Consistently, our RNA-seq analysis indicated that ST7 regulated the expression of actin cytoskeleton-related genes in pancreatic cancer. In particular, we identified that IQGAP1, a well-known cytoskeleton

regulator [19, 20], was downregulated by ST7 in pancreatic cancer. Intriguingly, pancreatic cancers often exhibit *KRAS* mutation and constitutive activation [10]. In addition to regulating the cytoskeleton, IQGAP1 is a scaffold protein modulating MAPK pathway activation [21]. Thus, targeting the IQGAP1 axis may represent a promising approach for pancreatic cancer treatment. In this study, we found that the ST7/IQGAP1 axis plays a critical role in pancreatic cancer progression; nevertheless, the mechanism of how ST7 inhibits IQGAP1 requires further investigation.

MIB1 contains multiple RING domains and functions as an E3 ubiquitin ligase, regulating several cellular processes [5]. Notably, MIB1 binds the intracellular tails of Notch ligands, promoting their ubiquitination necessary for Notch signaling activation [5]. Given the important role of the Notch pathway in modulating tumor growth, cancer metastasis, and the tumor microenvironment, MIB1-mediated ubiquitination of Notch ligands may affect all these tumor characteristics [22–24]. For instance, MIB1 has been shown to ubiquitinate JAG1 and activate Notch signaling in breast cancer [25]. Additionally, MIB1 has been implicated in the pathogenesis of spinal muscular atrophy by regulating cellular senescence and degrading motor neuron (SMN) [26]) and Werner syndrome (WRN) protein [27]. Recently, Fu et al. reported that MIB1 enhances pancreatic cancer growth and regulates gemcitabine-resistance by activating β-catenin signaling [7]. Nonetheless, the precise mechanisms of how MIB1 activates β-catenin is still unknown. Our data demonstrated that MIB1 exerted oncogenic functions in pancreatic cancer. Importantly, we identified ST7 as a novel substrate of MIB1 in pancreatic cancer. Although the c-Myc-dependent $CRL4^{DCAF4}$ E3 ligase has been shown to mediate ST7 degradation in colitis-associated cancer [28], the post-translational modifications of ST7 in pancreatic cancer remain unknown. In this study, we identified that by inducing ST7 degradation, MIB1 increases IQGAP1 expression and promotes pancreatic cancer progression.

In conclusion, our data suggest that MIB1 overexpression promotes pancreatic cancer progression by targeting ST7 for degradation. Furthermore, we identified ST7 as a tumor suppressor in pancreatic cancer, negatively regulating IQGAP1 expression. Therefore, the MIB1/ST7/IQGAP1 signaling axis plays a crucial role in pancreatic cancer cells progression, and inhibiting MIB1 may improve the survival of pancreatic cancer patients.

Abbreviations

MIB1: Mind bomb 1; ST7: Suppressor of tumorigenicity 7 protein; IQGAP1: IQ motif containing GTPase activating protein 1; SMN: Senescence and degrading motor neuron; WRN: Werner syndrome; IP: immuno-precipitated.

Declarations

Ethical Approval and Consent to participate

The study was conducted in accordance with the principles of the Declaration of Helsinki principles. It was approved by the Animal Use and Care Committees at Tongji Medical College, Huazhong University of Science and Technology.

Competing Interests

The authors have declared that no competing interest exists.

Funding

This work was supported by grants from the Chinese National Natural Science Foundation Grant No. 81572436 (T.L.).

Author Contributions

TL and XJ conceived and designed the study. TL and ZB contributed to carry out the experiments. XC contributed to data analysis. XC and TL provided clinical samples and clinical information.XC wrote the manuscript. XJ supervised the research. All authors read and approved the final manuscript.

Acknowledgement

Not applicable.

Consent for publication

All subjects have written informed consent.

Availability of data and materials

The datasets used and/or analyzed during the current study are available from the corresponding authors (Xin Jin, jinxinunion@hust.edu.cn) on reasonable request.

References

1. Ansari, D.; Tingstedt, B.; Andersson, B.; Holmquist, F.; Sturesson, C.; Williamsson, C.; Sasor, A.; Borg, D.; Bauden, M.; Andersson, R., Pancreatic cancer: yesterday, today and tomorrow. *Future Oncol* **2016,***12* (16), 1929-46.

2. Burrell, R. A.; McGranahan, N.; Bartek, J.; Swanton, C., The causes and consequences of genetic heterogeneity in cancer evolution. *Nature* **2013,***501* (7467), 338-45.
3. Yabar, C. S.; Winter, J. M., Pancreatic Cancer: A Review. *Gastroenterol Clin North Am* **2016,***45* (3), 429-45.
4. Kamisawa, T.; Wood, L. D.; Itoi, T.; Takaori, K., Pancreatic cancer. *Lancet* **2016,***388* (10039), 73-85.
5. Guo, B.; McMillan, B. J.; Blacklow, S. C., Structure and function of the Mind bomb E3 ligase in the context of Notch signal transduction. *Curr Opin Struct Biol* **2016,***41*, 38-45.
6. Cajanek, L.; Glatter, T.; Nigg, E. A., The E3 ubiquitin ligase Mib1 regulates Plk4 and centriole biogenesis. *J Cell Sci* **2015,***128* (9), 1674-82.
7. Fu, X.; Tang, N.; Xie, W.; Mao, L.; Qiu, Y., Mind Bomb 1 Promotes Pancreatic Cancer Proliferation by Activating beta-Catenin Signaling. *J Nanosci Nanotechnol* **2020,***20* (12), 7276-7282.
8. Collins, M. A.; Pasca di Magliano, M., Kras as a key oncogene and therapeutic target in pancreatic cancer. *Front Physiol* **2013,***4*, 407.
9. Abel, A. M.; Schuldt, K. M.; Rajasekaran, K.; Hwang, D.; Riese, M. J.; Rao, S.; Thakar, M. S.; Malarkannan, S., IQGAP1: insights into the function of a molecular puppeteer. *Mol Immunol* **2015,***65* (2), 336-49.
10. Jin, X.; Pan, Y.; Wang, L.; Ma, T.; Zhang, L.; Tang, A. H.; Billadeau, D. D.; Wu, H.; Huang, H., Fructose-1,6-bisphosphatase Inhibits ERK Activation and Bypasses Gemcitabine Resistance in Pancreatic Cancer by Blocking IQGAP1-MAPK Interaction. *Cancer Res* **2017,***77* (16), 4328-4341.
11. Jin, X.; Fang, R.; Fan, P.; Zeng, L.; Zhang, B.; Lu, X.; Liu, T., PES1 promotes BET inhibitors resistance and cells proliferation through increasing c-Myc expression in pancreatic cancer. *J Exp Clin Cancer Res* **2019,***38* (1), 463.
12. Fan, P.; Zhao, J.; Meng, Z.; Wu, H.; Wang, B.; Wu, H.; Jin, X., Overexpressed histone acetyltransferase 1 regulates cancer immunity by increasing programmed death-ligand 1 expression in pancreatic cancer. *J Exp Clin Cancer Res* **2019,***38* (1), 47.
13. Hooi, C. F.; Blancher, C.; Qiu, W.; Revet, I. M.; Williams, L. H.; Ciavarella, M. L.; Anderson, R. L.; Thompson, E. W.; Connor, A.; Phillips, W. A.; Campbell, I. G., ST7-mediated suppression of tumorigenicity of prostate cancer cells is characterized by remodeling of the extracellular matrix. *Oncogene* **2006,***25* (28), 3924-33.
14. Lu, C.; Xu, H. M.; Ren, Q.; Ao, Y.; Wang, Z. N.; Ao, X.; Jiang, L.; Luo, Y.; Zhang, X., Somatic mutation analysis of p53 and ST7 tumor suppressor genes in gastric carcinoma by DHPLC. *World J Gastroenterol* **2003,***9* (12), 2662-5.
15. Yoshimura, S.; Yamada, T.; Ohwada, S.; Koyama, T.; Hamada, K.; Tago, K.; Sakamoto, I.; Takeyoshi, I.; Ikeya, T.; Makita, F.; Iino, Y.; Morishita, Y., Mutations in the ST7/RAY1/HELG locus rarely occur in primary colorectal, gastric, and hepatocellular carcinomas. *Br J Cancer* **2003,***88* (12), 1909-13.
16. Zenklusen, J. C.; Conti, C. J.; Green, E. D., Mutational and functional analyses reveal that ST7 is a highly conserved tumor-suppressor gene on human chromosome 7q31. *Nat Genet* **2001,***27* (4), 392-8.

17. Wang, S.; Mori, Y.; Sato, F.; Yin, J.; Xu, Y.; Zou, T. T.; Olaru, A.; Kimos, M. C.; Perry, K.; Selaru, F. M.; Deacu, E.; Sun, M.; Shi, Y. C.; Shibata, D.; Abraham, J. M.; Greenwald, B. D.; Meltzer, S. J., An LOH and mutational investigation of the ST7 gene locus in human esophageal carcinoma. *Oncogene* **2003,***22* (3), 467-70.
18. Charong, N.; Patmasiriwat, P.; Zenklusen, J. C., Localization and characterization of ST7 in cancer. *J Cancer Res Clin Oncol* **2011,***137* (1), 89-97.
19. Liu, Y.; Liang, W.; Yang, Y.; Pan, Y.; Yang, Q.; Chen, X.; Singhal, P. C.; Ding, G., IQGAP1 regulates actin cytoskeleton organization in podocytes through interaction with nephrin. *Cell Signal* **2015,***27* (4), 867-77.
20. Hedman, A. C.; Smith, J. M.; Sacks, D. B., The biology of IQGAP proteins: beyond the cytoskeleton. *EMBO Rep* **2015,***16* (4), 427-46.
21. Roy, M.; Li, Z.; Sacks, D. B., IQGAP1 binds ERK2 and modulates its activity. *J Biol Chem* **2004,***279* (17), 17329-37.
22. Kontomanolis, E. N.; Kalagasidou, S.; Pouliliou, S.; Anthoulaki, X.; Georgiou, N.; Papamanolis, V.; Fasoulakis, Z. N., The Notch Pathway in Breast Cancer Progression. *ScientificWorldJournal* **2018,***2018*, 2415489.
23. Meurette, O.; Mehlen, P., Notch Signaling in the Tumor Microenvironment. *Cancer Cell* **2018,***34* (4), 536-548.
24. Hossain, F.; Majumder, S.; Ucar, D. A.; Rodriguez, P. C.; Golde, T. E.; Minter, L. M.; Osborne, B. A.; Miele, L., Notch Signaling in Myeloid Cells as a Regulator of Tumor Immune Responses. *Front Immunol* **2018,***9*, 1288.
25. Izrailit, J.; Jaiswal, A.; Zheng, W.; Moran, M. F.; Reedijk, M., Cellular stress induces TRB3/USP9x-dependent Notch activation in cancer. *Oncogene* **2017,***36* (8), 1048-1057.
26. Kwon, D. Y.; Dimitriadi, M.; Terzic, B.; Cable, C.; Hart, A. C.; Chitnis, A.; Fischbeck, K. H.; Burnett, B. G., The E3 ubiquitin ligase mind bomb 1 ubiquitinates and promotes the degradation of survival of motor neuron protein. *Mol Biol Cell* **2013,***24* (12), 1863-71.
27. Li, M.; Liu, B.; Yi, J.; Yang, Y.; Wang, J.; Zhu, W. G.; Luo, J., MIB1-mediated degradation of WRN promotes cellular senescence in response to camptothecin treatment. *FASEB J* **2020**.
28. Liu, H.; Lu, W.; He, H.; Wu, J.; Zhang, C.; Gong, H.; Yang, C., Inflammation-dependent overexpression of c-Myc enhances CRL4(DCAF4) E3 ligase activity and promotes ubiquitination of ST7 in colitis-associated cancer. *J Pathol* **2019,***248* (4), 464-475.

Figures

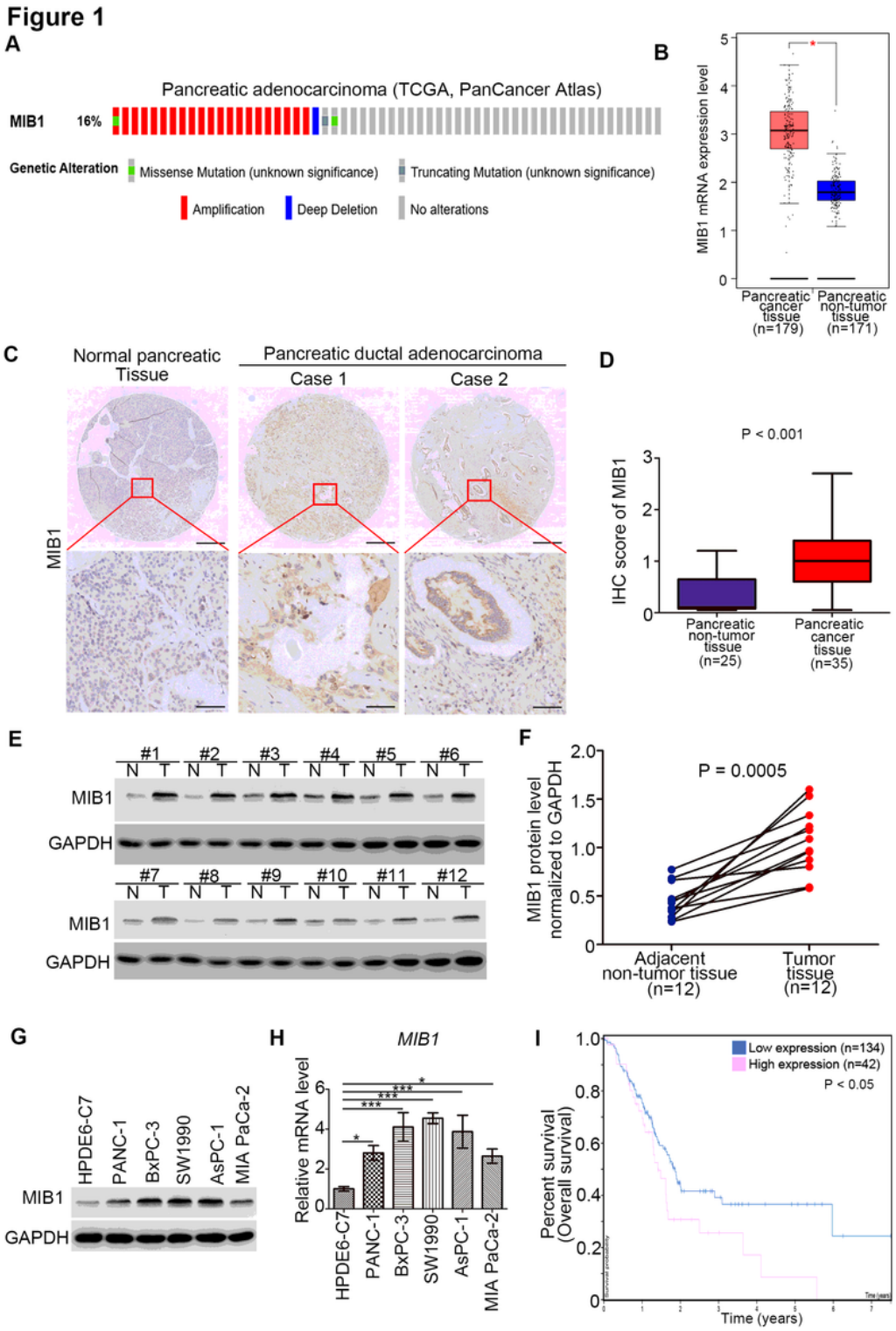

Figure 1

Aberrantly overexpressed MIB1 is associated with poor prognosis in pancreatic cancer. A, the mRNA expression level of MIB1 in the TCGA dataset (http://www.cbioportal.org/). B, analysis the mRNA expression level of MIB1 by using the GEPIA web tool (http://gepia.cancer-pku.cn/). C, representative IHC images stained with MIB1 in the tissue microarray. D, the protein levels of MIB1 from the tissue microarray were determined by IHC analysis, P value as indicated in the figure. E and F, the protein level of

MIB1 from pancreatic cancer tissues (n = 12) and adjacent normal pancreatic tissues (n = 12) was detected by Western blotting analysis, P = 0.0005. G and H, HPDE6-C7, PANC-1, BxPC-3, SW1990, AsPC-1 and MIA PaCa-2 were harvested for Western blotting analysis (G), RT-qPCR analysis (H). For the panel H, data presented as Mean ± SD with three replicates. *, P < 0.05; ***, P < 0.001. I, the overall survival rate in high/low MIB1 group was analyzed by the Human protein atlas (http://www.proteinatlas.org/), P < 0.05.

Figure 2

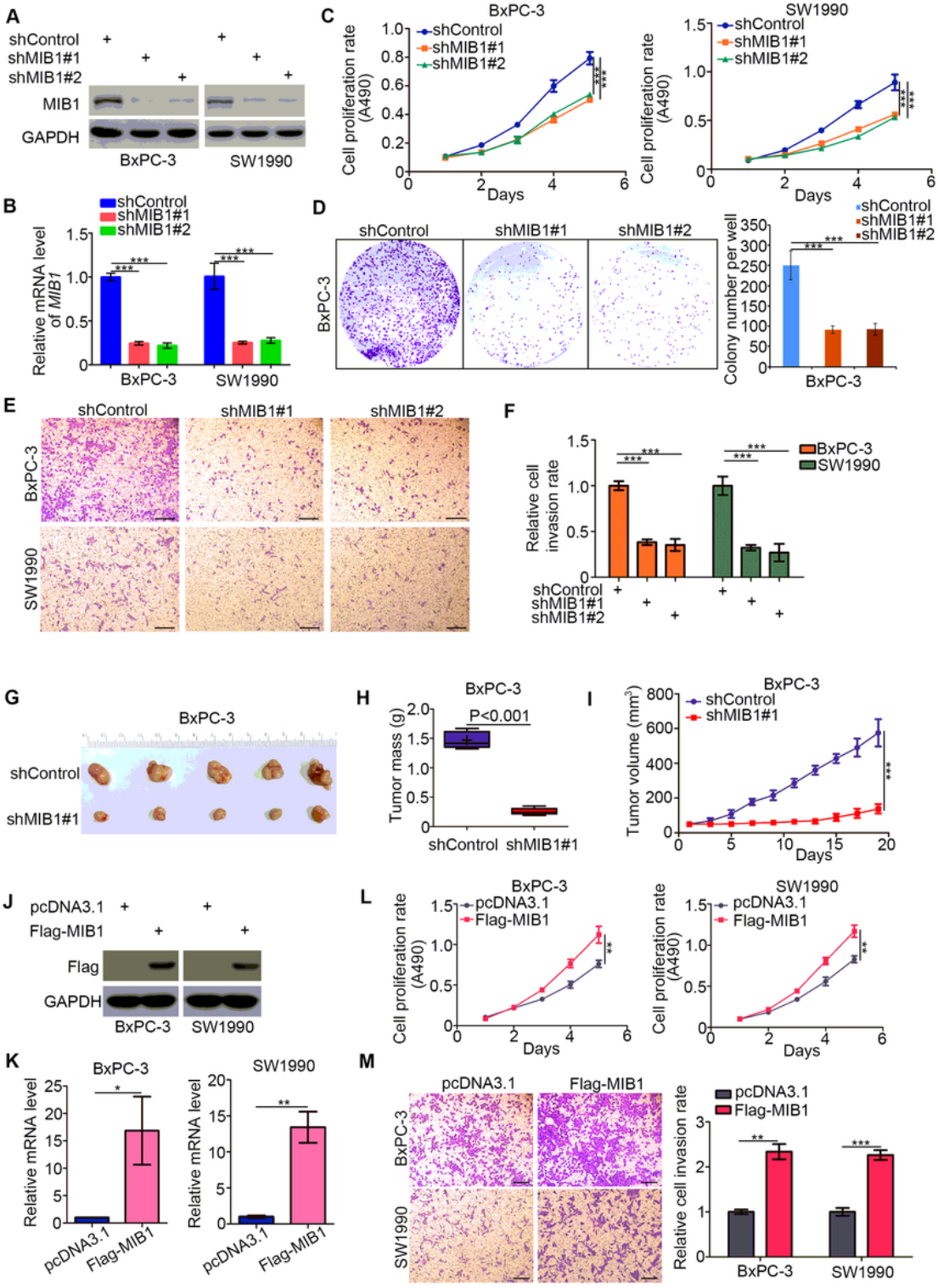

Figure 2

MIB1 is contribute to promoting pancreatic cancer cells progression A-F, BxPC-3 and SW1990 cells were infected with indicated shRNAs. 72 h post infection, cells were harvested for Western blotting analysis (A), RT-qPCR analysis (B), MTS assay (C), colony formation assay (D) and transwell assay (E). For the panel B-E, data presented as Mean ± SD with three replicates. ***, P < 0.001. G-I, BxPC-3 cells were infected with indicated shRNAs. After 72h puromycine selection, cells were harvested and subcutaneously injected into nude mice for xenografts assay. The image of tumor was shown in panel G. The tumor mass was demonstrated in panel H. The tumor growth curve was indicated in panel I. Data presented as Mean ± SD with five replicates. ***, P < 0.001. J-M, BxPC-3 and SW1990 cells were transfected indicated constructs. After 48 h, cells were harvested for Western blotting analysis (J), RT-qPCR analysis (K), MTS assay (L) and transwell assay (M). For the panel K-M, data presented as Mean ± SD with three replicates. ***, P < 0.001.

Figure 3

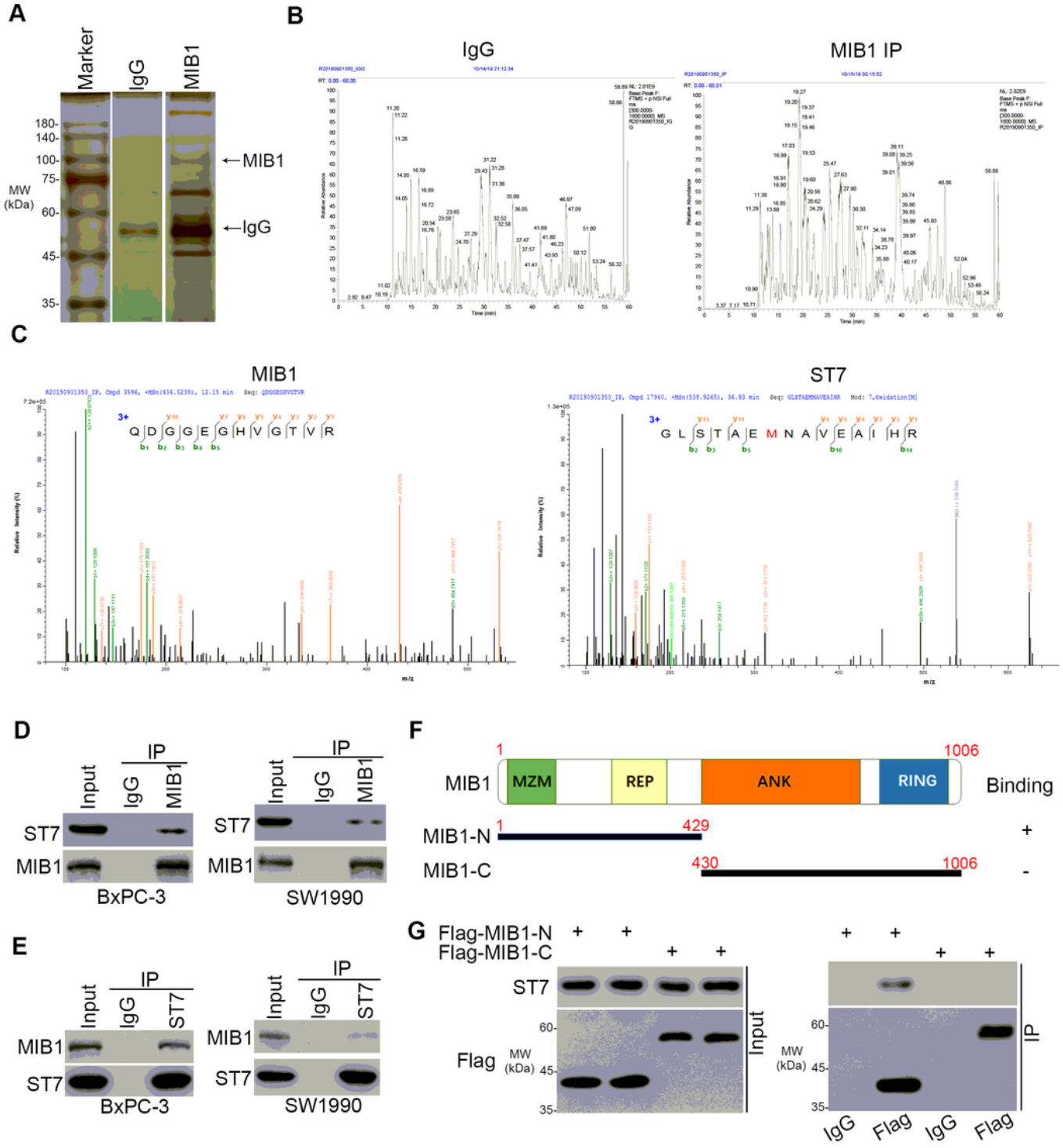

Figure 3

MIB1 interacts with ST7 in pancreatic cancer cells. A-C, the WCL of BxPC-3 cells were subjected to silver staining (B) and mass spectrometry with IgG and MIB1 antibodies (B and C). D and E, western blotting analysis of the whole cell lysates (WCL) of BxPC-3 and SW1990 cells. F, a schematic diagram depicting the domain of MIB1. G, Flag-MIB1-C and Flag-MIB1-N were translated in vitro, the immunoprecipiation was employed to examine the region of MIB1 binding with ST7.

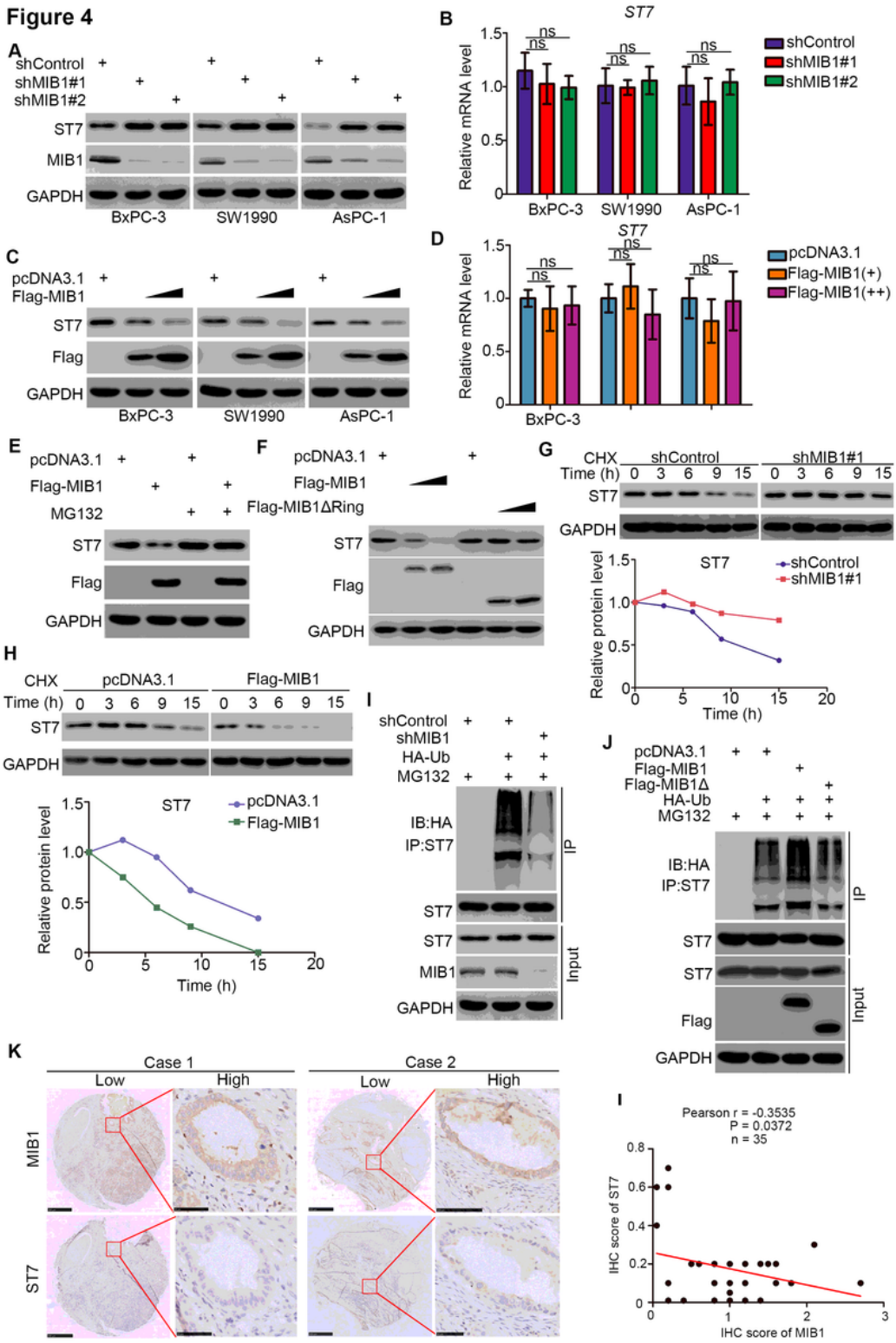

Figure 4

ST7 is a bona fide substrate of MIB1 in pancreatic cancer. A and B, the pancreatic cancer cell lines (BxPC-3, SW1990, AsPC-1) were infected with indicated shRNAs. 72 h post infection, cells were harvested for Western blotting analysis (A) and RT-qPCR analysis (B). Data presented as Mean ± SD with three replicates. ns, not significant. C and D, the pancreatic cancer cell lines (BxPC-3, SW1990, AsPC-1) were transfected with indicated constructs. After 48 h, cells were harvested for Western blotting analysis (C)

and RT-qPCR analysis (D). Data presented as Mean ± SD with three replicates. ns, not significant. E, BxPC-3 cells were transfected with indicated constructs. After 48 h, the WCL of BxPC-3 was subjected to Western blotting analysis. Cells were treated with or without 20 μM of MG132 for 8 h before harvested. F, BxPC-3 cells were transfected with indicated constructs. After 48 h, the WCL of BxPC-3 was subjected to Western blotting analysis. G, BxPC-3 cells were infected with indicated shRNAs. After 72 h, cells were treated with Cycloheximide (CHX) and cells were collected for Western Blotting analysis at different time points. H, BxPC-3 cells were transfected with indicated plasmids. After 48 h, cells were treated with Cycloheximide (CHX) and cells were collected for Western Blotting analysis at different time points. I, BxPC-3 cells were infected with indicated plasmids. 72 h post-infection, cells were collected for Western Blotting analysis after treated with MG132 for 8 h. J, BxPC-3 cells were transfected with indicated plasmids. After 48 h, cells were collected for Western Blotting analysis after treated with MG132 for 8 h. K and L, the tissue microarray of pancreatic cancerwas stained with MIB1 and ST7 respectively. The typical IHC images stained with MIB1 and ST7 were shown in panel K. The correlation of these two proteins was shown in panel L, the P value was indicated in the figure.

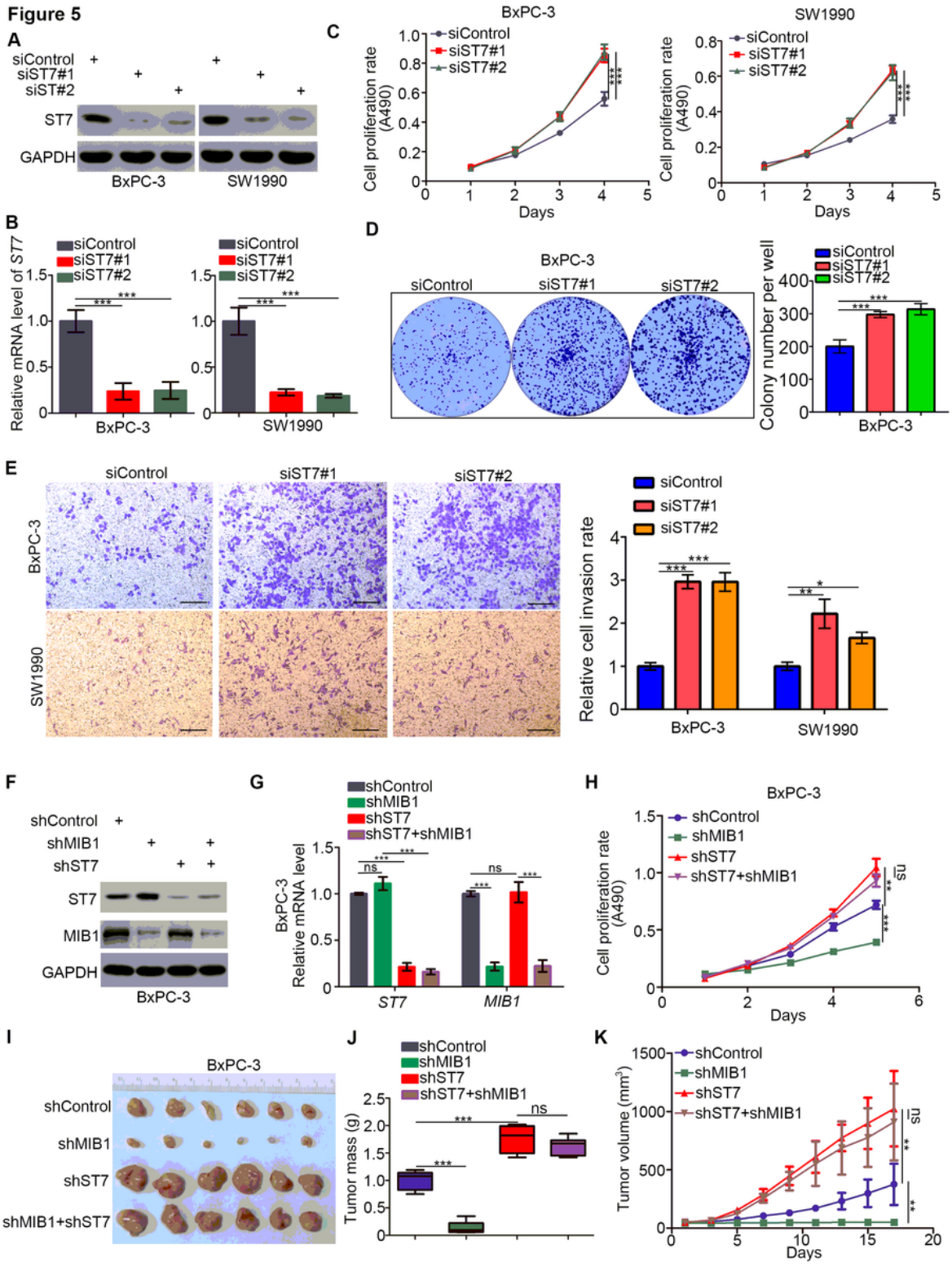

Figure 5

ST7 is the key mediator for MIB1 induced pancreatic cancer cells progression A-E, BxPC-3 and SW1990 cells were infected with indicated shRNAs. 72 h post infection, cells were harvested for Western blotting analysis (A), RT-qPCR analysis (B), MTS assay (C), colony formation assay (D) and transwell assay (E). For the panel B-E, data presented as Mean ± SD with three replicates. *, P < 0.05; **, P < 0.01; ***, P < 0.001. F and K, BxPC-3 were infected with indicated shRNAs. 72 h post infection and puromycine

selection, cells were harvested for Western blotting analysis (F), RT-qPCR analysis (G), MTS assay (H) and xenografts assay (I-K). For the panel G and H, data presented as Mean ± SD with three replicates. ns, not significant; **, P < 0.01; ***, P < 0.001. The image of tumor was shown in panel I. The tumor mass was demonstrated in panel J. The tumor growth curve was indicated in panel K. Data presented as Mean ± SD with five replicates. ns, not significant; **, P < 0.01;***, P < 0.001.

Figure 6

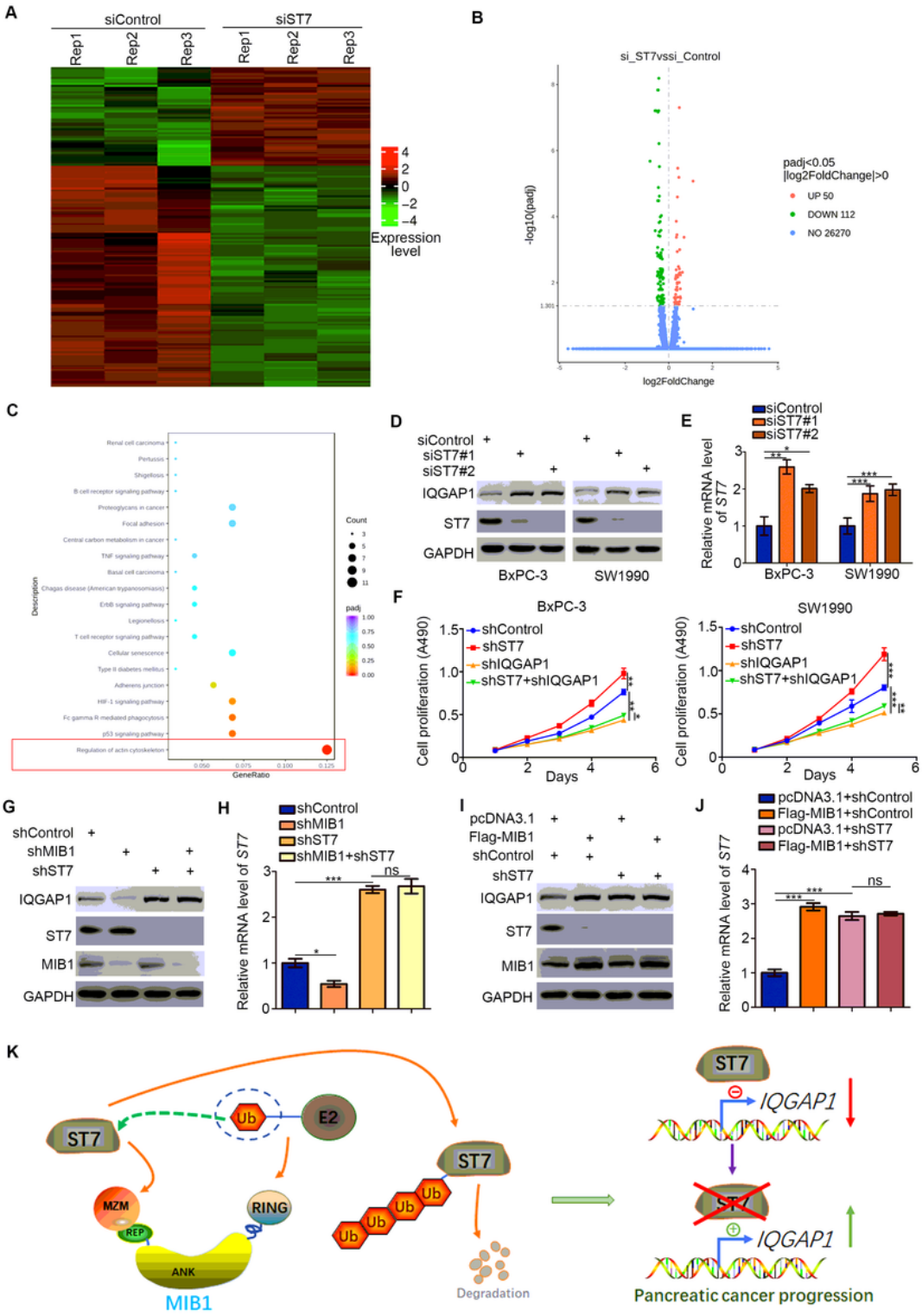

Figure 6

The MIB1/ST7/IQGAP1 signaling axis increases pancreatic cancer proliferation A-C, BxPC-3 cells were transfected with indicated constructs for 48h. Cells were subjected to RNA-seq analysis (A and B) and subsequent KEGG pathway enrichment (C). D and E, BxPC-3 and SW1990 cells were transfected with indicated constructs. After 48 h, cells were harvested for Western blotting analysis (D) and RT-qPCR analysis (E). Data presented as Mean ± SD with three replicates. *, P < 0.05; **, P < 0.01; ***, P < 0.001. F, BxPC-3 and SW1990 cells were infected with indicated shRNAs. 72 h post infection, cells were harvested for MTS assay. Data presented as Mean ± SD with three replicates. *, P < 0.05; **, P < 0.01; ***, P < 0.001. G and H, BxPC-3 cells were infected with indicated shRNAs. 72 h post infection, cells were harvested for Western blotting analysis (G) and RT-qPCR analysis (H). Data presented as Mean ± SD with three replicates. ns, not significant; *, P < 0.05; ***, P < 0.001. I and J, BxPC-3 cells were infected with indicated shRNAs. After 48 h, cells were transfected with indicated plasmids for other 24 h. cells were harvested for Western blotting analysis (I) and RT-qPCR analysis (J). Data presented as Mean ± SD with three replicates. ns, not significant; ***, P < 0.001. K, a hypothesis model depicting that abnormally up-regulated MIB1 degrades ST7 to increase IQGAP1 expression and promotes pancreatic cancer progression.

Supplementary Files

This is a list of supplementary files associated with this preprint. Click to download.

- TableS1.massspectrometryofMIB1.xlsx
- TableS2.RNAseqofST7.xlsx
- Supplementaryinformation.docx